Biomedical Physics & Engineering Express

ENDORSED BY IPEM Institute of Physics and Engineering in Medicine

ACCEPTED MANUSCRIPT

Real time remodeling of cellular morphology using optical imprinting of cell-culture substrates

To cite this article before publication: Maryam Ali *et al* 2019 *Biomed. Phys. Eng. Express* in press https://doi.org/10.1088/2057-1976/aafc8e

Real-time remodeling of cellular morphology using optical imprinting of cell-culture substrates

Maryam Ali and Jason B. Shear*

Department of Chemistry, 1 University Station A5300,

The University of Texas at Austin, Austin, TX 78712

Abstract

Development of materials that can dynamically alter the topographic experience of cultured cells is key to accurately modeling in vivo processes such as tissue development and repair. Current technologies have largely focused on smart substrate materials that can be programmed to undergo topographical transformations in the presence of adhered cells, but such materials provide limited spatiotemporal resolution and generally are triggered by undesirable changes to environmental conditions. Here, we present an approach for investigating cellular responses to dynamic topographical cues in which multiphoton photochemistry is used to remotely imprint a substrate with arbitrary topographical patterns in real time (i.e., in the presence of adherent cells). In these studies, fibroblastic NIH3T3 cells were plated on a planar protein hydrogel substrate, where they generally established stereotypical polygonal morphology before the underlying substrate was dynamically transformed to a grooved topography. Elongation and alignment of cells exposed to low-micrometer-pitch grooves imprinted in this manner occurred less rapidly than for cells directly deposited on substrates having pre-formed grooves. Further, cell alignment on dynamically imprinted grooves was notably delayed relative to elongation, suggesting that the structural attributes of a cell at the time it first experiences a grooved topography may differentially influence these two processes. This minimally invasive approach for subjecting cells to dynamic topographical experiences represents a versatile means to model evolving conditions within in vivo systems and to systematically explore mechanisms of cellular morphology and behavior.

1. Introduction

Phenotypic attributes of adherent cells can be dramatically influenced by physical and chemical interactions with both the extracellular matrix (ECM) and neighboring cells. Cellular responses to ECM topography have been investigated extensively *in vitro* for adherent cells on surfaces containing numerous feature types [1]. Grooves, in particular, are capable of promoting a wide range of cell responses, including elongation, alignment, directed motility, and directed outgrowth. The type and extent of such behaviors depend on both cell type and groove dimensions [2], as well as substrate characteristics such as stiffness (e.g., Young's modulus), hydrophobicity, and functional-group display [3, 4].

Adherent cells bind to many substrates, in part, through focal adhesions that can transduce extracellular cues as integrated cytosolic signaling patterns. Such signaling can promote, for example, extension and retraction of protrusions through cytoskeletal assembly/disassembly [1]. When plated on grooves of appropriate lateral and vertical dimensions, cells preferentially form focal adhesions parallel to (rather than across) grooves [2], eliciting heterogeneous intracellular signaling and a consequent transition to bipolar morphology aligned with the groove long axis [5-7].

Cells *in vivo* exist within dynamic environments whose topographies and mechanical properties transition over time. Remodeling of the ECM and neighboring-cell arrangements occurs in normal development, wound/burn healing, and various disease states [8] – environmental changes that have been shown to affect morphology and overall cell fate [9-11]. Such responses, however, have been difficult to investigate using model in vitro systems, as methods for non-invasively modifying cellular physical environments in real time with sufficient speed and control have proved elusive.

Various groups have attempted to address this need by developing substrate materials that undergo stimuli-dependent topographical changes. Shape-memory polymers (SMPs), for example, can be cast in their thermodynamically stable configurations, then molded temporarily into metastable shapes [12]. An environmental switch can then be used to revert a strained SMP at a desired time to the configuration defined during its casting. Although this approach can be used to study adherent-cell response to topographical stimuli, SMPs do not provide flexibility for arbitrarily specifying the nature of

topographical changes on-the-fly, during the course of an experiment. Moreover, SMPs most commonly are triggered via temperature jumps (e.g., from 30°C to 37°C), perturbations known to affect various cellular behaviors [13]. Several other strategies for altering topography on demand have been developed that avoid the need for temperature steps, but each are limited in key ways. For example, laser-induced ablation of surface material can be used to alter cell-culture topography, but is highly disruptive when performed at existing cell-substrate interfaces [14]. Alternatively, externally applied forces have been used to induce wrinkles in various material types that promote cell alignment [15, 16], but such an approach provides limited control over topographical features and lacks the spatial resolution necessary to selectively modify substrates beneath specific, targeted cells.

To address these key limitations, our lab has developed a laser-scanning strategy for modifying topographic landscapes [17]. In this approach, cell-culture hydrogel substrates composed of partially crosslinked proteins and a photosensitizer are scanned with tightly focused femtosecond laser light to promote additional crosslinking via multiphoton excitation of the photosensitizer within a defined plane of the hydrogel. By exposing hydrogels to specified scan patterns, and repeating this process at multiple scan focal planes within the substrate, arbitrarily defined topographical features can be projected onto the hydrogel surface without disrupting cell-substrate adhesion or compromising cell viability, all without subjecting cells to varying temperatures (or other environmental conditions). Importantly, such features have the capability to be customized on-the-fly in response to observed cellular behavior.

Here, we report the ability to exert dynamic control over cellular morphology using this *in situ* hydrogel imprinting technique. After plating and adhesion of cells onto hydrogel substrates composed of crosslinked gelatin/bovine serum albumin (BSA), microscale grooves are imprinted at the cell-substrate interface to modify morphology and orientation of mouse embryonic NIH3T3 fibroblast cells in real time (Figure 1; Supporting Movie S1), revealing significant differences in the time scales of alignment for cells exposed to grooves after substrate adhesion versus those plated directly on grooved substrates. NIH3T3 cells represent rational proof-of-concept model systems for examining topographic effects of imprinting due to the extensive use of fibroblastic cells in studies directed at understanding the impact of grooves on cellular alignment, elongation, and related behaviors [18, 19]. This approach

provides unprecedented capabilities for investigating cellular responses to real-time topographical perturbations under minimally invasive conditions, enabling, for example, systematic studies on the time course of morphologic responses as a function of initial cellular states.

2. Materials and methods

2.1. Hydrogel reagent solution

Photosensitizer (15 mM Rose Bengal, RB; Sigma-Aldrich, St. Louis, MO) initially was dissolved in pH 7.2 phosphate-buffered saline (PBS; Pierce BupH Phosphate Buffered Saline Packs, ThermoFisher Scientific, Carlsbad, CA). BSA (300 mg; Equitech-Bio, Kerrville, TX) was dissolved in 1 mL of photosensitizer solution and the solution was warmed to 60°C. Type A porcine gelatin (100 mg; Sigma-Aldrich, St. Louis, MO) was dissolved in the warmed RB-BSA solution, and the resultant warmed RB-BSA-gelatin solution was applied to a coverglass surface (Mattek glass-bottom well, #1, Ashland, MA) and cooled to a gel at ambient temperature for use in hydrogel fabrication.

2.2. Micro-3D-printing instrumentation

Hydrogel substrates for cell culture were fabricated using multiphoton lithography (MPL). Instrumentation for MPL was similar to that reported previously [20]. Briefly, output from a mode-locked titanium-sapphire (Ti:S) laser (Model 900 Mira, Coherent Inc., Santa Clara, CA) tuned to 740 nm was scanned in a raster pattern using a scanning galvo mirror system (Thor Labs, Newton, NJ). A series of lenses and mirrors (Thor Labs, Newton, NJ) was used to expand the laser beam and the scan area, eventually focusing the beam onto the face of a digital micromirror device (DMD) from a re-purposed digital projector (BenQ MP510 DLP Projector, BenQ, Costa Mesa, CA) which served as a dynamic mask for the raster-scanned beam. The masked scan pattern was focused through a high-power objective (60x oil, 1.4 NA, Nikon Instruments, Melville, NY) on an inverted microscope (TE-2000, Nikon Instruments, Melville, NY), and a piezo-controlled nanopositioner (E-710, Physik Instrumente, Auburn, MA) was used to translate the stage along the optical axis.

2.3. Fabrication of hydrogel tile arrays

Laser powers typically were adjusted to ~35 mW at the objective back aperture to promote gelatin and BSA crosslinking via two-photon excitation of RB in a process likely promoted by singlet

oxygen mechanisms involving histidine and other residues [21-23]. The laser beam was raster-scanned in a given plane with fast-axis and slow-axis scan velocities of 68 mm s^{-1} and 25 μm s^{-1}, respectively. Scan regions within reagent solution were limited to relatively small areas (70 μm × 70 μm), making it necessary to laterally "tile" together multiple scan regions to produce a tile-array cell-culture substrate.

Each tile was fabricated as a sequence of vertically stacked fabrication planes. In this process, an initial plane located at a height nominally 10 μm above the coverglass surface was raster scanned to crosslink BSA/gelatin in the reagent gel into a sheet. Following this initial scan, the coverglass surface was translated in 1-μm increments (vertically away from the objective), and the focused beam was raster scanned in each new focal plane until a (nominally) 10-μm-thick printed tile was anchored to the coverglass surface. To produce a cell-culture substrate, an arrangement of adjacent tiles (with a lateral overlap of ~2 μm) was printed to form a hydrogel tile array having a surface area of ~0.5 mm^2. After MPL was completed, unscanned reagent was rinsed away using PBS warmed to 60°C. Additional RB photosensitizer was extracted by soaking the tile array overnight in a 50% v/v ethanol/water solution. To prepare substrates for quantitative studies on imprinting cellular alignment/elongation, tile arrays subsequently were loaded overnight in a 5-mM solution of the biocompatible photosensitizer eosin Y (eosin; MP Biomedicals, LLC, Solon, OH) in PBS, and stored at least overnight and up to a period of 2 days until use. For the qualitative study shown in Figure 1, the BSA-gelatin tile array were derivatized with eosin-ITC to enhance imprinting capacity.

2.4. NIH3T3 cell cultures

NIH3T3 cells (CRL-1658, ATCC, Mannasas, VA) were used from passages 7 to 20 after thawing and growing in complete media (DMEM with high glucose, L-glutamine, and sodium pyruvate, and 10% bovine calf serum; Hyclone, Thermo Fisher Scientific, Waltham, MA) in a 5% CO_2 atmosphere. For microscope observations outside a 5% CO_2 atmosphere, cells were maintained in plating medium composed of Leibovitz's L-15 medium (Hyclone) with 1% bovine calf serum and 1% penicillin-streptomycin (GIBCO, Grand Island, NY). Cells were plated on tile arrays at densities of ~5 x 10^3 cells cm^{-2}. Imaging was performed using red-light illumination to minimize photosensitizer excitation.

2.5. Imprinting topographical patterns on hydrogel tile arrays

Masks were designed and displayed on the DMD using presentation software (Powerpoint, Microsoft, Redmond, WA) with display patterns corresponding to desired imprint patterns. Laser powers and scan speeds for imprinting were the same as those used in fabrication of tile arrays. Beginning at a height H_0 above the glass surface, the laser voxel was raster-scanned in horizontal planes through the material, with 1-μm downward (relative to the coverslip) increments between each scan plane, until a plane was reached that was nominally at least 3 μm into the coverslip glass. For imprinting that relied on multiple scan passes, the laser voxel was returned to height H_0 and the process was repeated. For hydrogels that were "pre-imprinted" with patterns before cell application, patterned tile arrays were stored in eosin solution to maintain their hydration as well as a photosensitizer concentration comparable to that of tiles used for in situ imprinting.

2.6. Characterizing dimensions of imprinted tiles

Negative-space confocal imaging was used to measure surface feature and tile lateral extent dimensions. Here, imprinted tiles were submersed in a solution of FITC-conjugated dextran molecules (2 MDa; FD2000; Sigma-Aldrich). Imprinted microstructures were imaged using confocal microscopy (Leica SP2 AOBS; Leica Microsystems, Buffalo Grove, IL), with tiles appearing as lower-fluorescence signal regions relative to intensely fluorescent fluorescein-dextran solution in the surrounding volume. Samples were excited using a 488-nm line from an argon-ion laser source focused through a 63X (HCX APO, 1.4NA) oil objective. Emitted light was collected in a nominal window of 496–675 nm. Three-dimensional images were captured as z-series stacks at a nominal resolution of 465 nm per pixel in the radial dimensions, while optical sections along the axial dimension were collected using stage increments of 115 nm. Orthogonal projections of confocal images were computed using FIJI imaging software [24].

2.7. Quantifying cell elongation and alignment to grooves

In studies where cells were plated onto pre-imprinted tile arrays, experimental time was defined such that cells settled on grooved surfaces at time t = 0.0 h. (indicated by cells entering the same plane of focus as the upper surface of tile array/solution interface). For dynamic substrates, the end of the

imprinting process was defined as time t = 0.0 h. Cells typically were imaged every 5 min over a 24 h. period using a Zeiss inverted microscope in brightfield mode outfitted with a scientific-grade charge-coupled device camera (CoolSNAP fx, Photometrics, Tuscon, AZ). A shutter (VS25, Uniblitz, Rochester, NY) limited illumination times to 200 ms per image. Frames corresponding to t = 4.6 h., 11.0 h., and 16.3 h. were extracted in each experimental data set for analysis.

Cells were individually tracked over the entire observation period, allowing cells that migrated away from their respective surface types (from grooved to planar surfaces, and vice versa) to be excluded from analysis. Forty cells were analyzed on pre-imprinted surfaces and 32 cells were analyzed on dynamically imprinted surfaces. Each cell outline was manually traced in FIJI, and binary image files were created of cell shapes. The “Analyze Particles” tool was applied with a size range of (100 to ∞) and a circularity range of (0.00 to 1.00). The EllipseFitter.java routine was used to determine best-fit ellipses with first and second moments matching each cell shape [25]. For each cell, the aspect ratio (AR; the ratio of the major axis of the ellipse to the minor axis) and the alignment angle (AA; the angle between the major axis of the ellipse and the groove axis) were measured. Possible alignment angles range from -90° to +90°, with a 0° value indicating that a cell major axis was parallel to grooves.

3. Results and discussion

3.1. Imprinting Hydrogel Substrates

Numerous studies have described multiphoton excitation of photosensitizers to promote three-dimensionally localized protein crosslinking [26-29]. By scanning the focus of a femtosecond laser beam in three dimensions, this process can be used to create microscopic protein-based hydrogels. Notably, when such hydrogels are re-scanned with specified patterns using same laser beam used for fabrication, site-specific contraction within the hydrogel matrix can be used to produce de novo topographical features on the substrate surface (Figure 1) [17]. While detailed mechanisms of this process are still under investigation, re-scanning appears to promote additional hydrogel crosslinking causing focal contraction that projects corresponding impression features onto the hydrogel surface.

To optimally influence phenotypic properties of surface-adherent cells, we characterized the capacity to tune hydrogel imprinting based on scan parameters. Here, we fabricated tiles with nominal dimensions of 70 μm (width) × 70 μm (length) × 10 μm (height). Entire tiles were contracted by scanning uniformly one or more times through their volume (i.e., layer-by-layer through their entire height) with the focused Ti:S laser beam. Pre- and post-imprinting tile dimensions, including heights, were measured via negative-space confocal imaging.

In these measurements, the initial scan plane was nominally 14 μm above the coverslip surface. Table 1 (left) shows that the first scan through a tile produced the most dramatic effect, a decrease in height of ~30%, with a second scan yielding a somewhat smaller height decrease. Subsequent scans did not cause a significant further decrease in tile height, and it was therefore deemed unnecessary in groove imprinting studies to scan more than twice (termed "double scanning") for the purpose of increasing trough depth.

In some circumstances where the top surface of an imprinting substrate supports photosensitive biological or chemical materials (e.g., living cells, proteins), it may be desirable to promote topographical modification by initiating an imprinting scan at a plane below the top surface of a tile (i.e., within the imprinting material), and scanning through a downward sequence of planes until the coverglass is reached (or until a desired feature depth is produced). We therefore explored the effects of starting imprinting scans at different initial height positions.

As defined above, the value, H_0, represents the distance of this initial scan plane from the coverglass surface that anchors the imprinting material. We further define H_i as the initial height of a tile, and H_f as the final height of a tile when imprinting is completed. To quantify the effects of varying H_0 on imprinting, a set of 24 tiles having a mean initial height of 9.4 μm were each double-scanned using one of four H_0 values (8, 10, 12, and 14 μm), with each H_0 value therefore represented by six replicates. The results are summarized in Table 1 (right).

When H_0 was less than H_i, as is the case when H_0 = 8 μm, only a portion of the tile (i.e., that which is below H_0) was scanned on the initial scan. (Note that for multi-scan processing, this condition is not necessarily maintained on subsequent scans: since tile height decreases with each scan iteration,

interim tile height may become less than H_0). In contrast, when H_0 is greater than H_i, the entire tile height is scanned during all imprinting scans. Thus, for the three highest scan start positions, H_0 = 10, 12, and 14 μm, this simple picture predicts that tiles scanned with each of these initial scan positions should decrease to a uniform H_f, a result that was observed within experimental error.

We performed additional studies to evaluate effects of varying scan parameters on dimensions of grooves imprinted using dynamic-mask patterning. Effects of changing H_0 and number of scans on trough depth (the difference between heights measured at the ridge surface and trough surface) were assessed by imprinting 70 μm × 70 μm × 10 μm tiles with grooves having 5-μm-wide ridges and 15-μm-wide troughs (designated "R5/T15"). Double-scans were performed in all instances, as pilot studies indicated that a single scan did not imprint troughs deep enough to align cells, while a third scan did not provide a significant change in depth over two scans. H_0 was varied from 8 to 14 μm as before, and resulting groove depths were determined via negative-space confocal imaging. These measurements are summarized in Table 2.

The height change when producing grooves is generally smaller than the corresponding change in height of a tile scanned across its full area [Table 2, Table 1 (right)]. This disparity likely can be attributed to the non-zero shear modulus of the printed material: when imprinted regions contract, they experience shear stress from surrounding non-imprinted regions that opposes downward contraction, reducing the overall height change of the imprinted region.

Based on the measurements in Table 2 and initial studies examining cell alignment, H_0 was set to 12 μm for cellular imprinting studies, as it provided reproducible grooves capable of stimulating cellular morphological changes while only exposing cells briefly through a portion of their thickness. Using this protocol, cells maintained high viability, with no discernible effects on survival or behavior in the ~20-h. period following scanning on hydrogel tiles. Further, cells plated on coverglass demonstrated high tolerance for exposure to laser scanning under the optical conditions of these studies, with essentially no apoptosis or necrosis observed when scanning cells multiple times in the substrate-cell interface plane. For all alignment studies on either static or dynamically formed grooves, we employed imprinting protocols that yielded surfaces having 5-μm-wide ridges and 15-μm-wide troughs that were

~2-μm deep, as cells plated on pre-formed grooves with narrower troughs (R5/T5 and R5/T10, ~2-μm trough depth) or shallower troughs (R5/T15, <1.5-μm depth) exhibited markedly less alignment.

3.2. Cells align to *in situ* dynamically imprinted grooves

Efforts to understand cell elongation and alignment have focused extensively on fibroblasts and related cells [30], particularly the NIH3T3 line, which has been established as a well-validated model for investigating contact guidance and other surface-response behaviors [31]. Here, we seek to understand differences in how NIH3T3 cells perceive topographic features presented to the cellular membrane under two circumstances – either at the onset of cell-surface contact, or at later times after cells have fully adapted to an adherent phenotype on a planar surface. Toward this goal, a series of studies were undertaken in which NIH3T3 cells were plated on protein hydrogel tiles having either (1) pre-formed, "static" grooves (R5/T15, ~2-μm trough depth), or (2) naïve planar tiles that could be subsequently imprinted to dynamically modify substrate topography (in these studies, imposing the same groove dimensions as in (1)) while cells are already adherent.

Because the micro-3D-printing system we employ is limited to fabricating areas of approximately 70 μm × 70 μm, production of large imprintable culture surfaces required that substrates be formed by "quilting" together arrays of many tiles. Although overlapping edges did produce topographical seams (oriented at 45° to imprinted grooves), no discernible effects from seams were observed on NIH3T3 cell alignment.

Cells plated on pre-formed grooves typically responded in a manner consistent with previous reports using other materials [31-34], with cells adhering to the substrate, probing their surroundings through cyclical extensions and contractions of lamellipodia, and elongating principally in the groove dimension. At a molecular level, these actions have been shown to be mediated in part by rearrangement of microtubules and actin filaments [35], with focal adhesions forming on the ventral surfaces of cells, distributing predominantly along the groove axis [36]. Actin stress fibers anchored to the intracellular side of focal adhesions transduce intracellular cues, where integration of signals directs morphological transformation into a bipolar phenotype [5].

Cells plated on hydrogel tiles before dynamic imprinting initially encountered a planar surface with no strong directive cues, and as a result, typically were observed to extend their leading edges in an apparently random manner. For a large fraction of cells, competition between multiple leading edges produced a characteristic polygonal morphology with random orientation (Figure 2, left panel), consistent with previous reports [37, 38]. After allowing cells to adhere to planar surfaces for ~3 h., tile arrays were subjected to dynamically imprinting to produce grooves having 5-μm-wide ridges and 15-μm-wide troughs. Such in situ modification to hydrogel topography strongly biased cells to transition over a period of hours to a bipolar morphology with a high level of alignment to grooves (Figure 2, center and right panels; Supplemental Figure S1). Fluorescence microscopy revealed that for both pre-imprinted and dynamically imprinted grooved surfaces, actin fibers in bipolar cells also aligned parallel to grooves (data not shown). Cells plated on planar tile-array substrates that were not subjected to groove imprinting retained a polygonal morphology.

3.3. Cells on dynamic surfaces align more slowly than those on static grooved surfaces

To explore how the time course of phenotypic responses may differ when cells encounter either pre-formed grooves or grooves formed after cells have adhered to a planar substrate, we tracked alignment angles and aspect ratios for cells on each surface type. Individual cells were tracked over their entire history, and any cells that migrated away from their respective specified surface types were eliminated from analysis.

The imprinting process can be accomplished in as little as 2 min when relatively small regions of interest are targeted (i.e., a tile having 70 μm × 70 μm area), a rapid time scale that opens opportunities to investigate temporal characteristics of cellular alignment. In cases where large tile arrays are imprinted, imprinting may take tens of minutes or longer; because imprinting occurs in serial fashion across the substrate, different cells may initially experience topographical transitions at significantly different times. Such discrepancies could be minimized in future studies by, for example, using multiple scan beams in parallel [39].

To track the time course of cell alignment, we define t = 0.0 h. as the time that cells nominally began interaction with grooves. This time either represents the point at which plated cells first settled

on a grooved surface, or alternatively, when adherent cells experienced a change in the topography of their substrate from planar to grooved. As suggested above, for large dynamic surfaces, t = 0.0 h. is less precisely defined across a population, as different members of the population encountered grooves at different time points over an approximate 2-h. imprinting process. For practical considerations, we therefore define t = 0.0 h. for dynamic surfaces as the *end point* of the imprinting process, meaning that the groove-cell alignment time for a given cell was at least as long as the recorded alignment time.

Cell morphologies were characterized to provide metrics of alignment and elongation. Cells freshly plated on pre-formed grooves had uniformly round morphologies at t = 0.0 h. In contrast, at t = 0.0 on dynamic surfaces, cells were already adherent, and therefore, were generally polygonal, unelongated, and oriented randomly on the hydrogel surface. At t = 0.0 h. and later times on both surfaces, we approximated cell morphologies by best-fit ellipses, as demonstrated in previous reports [40]. Aspect ratios and alignment angles of cells were derived from these ellipses.

Cellular aspect ratio (AR) is used as a measure of elongation. In these studies, we considered a cell to be "elongated" if its AR was three times the AR of cells growing on a planar surface (determined to be 1.0 ± 0.3 at 6.5 h.). We therefore set a threshold for elongation at AR = 3. Cells plated on pre-formed grooves, being round, also had an AR ≈ 1 at t = 0.0 h.

The cellular alignment angle (AA) provides a gauge for how closely the long axis of an elongated cell aligns with the direction of grooves. By definition, AA = 0° when the long axis is parallel to grooves, and ±90° when it is perpendicular to grooves. When cell orientation is random, the magnitude of the AA has an expected mean value of 45°. In the current studies, cells are considered to be "aligned" when $|AA| \leq 15°$, a criterion consistent with previous reports [41]. In addition, assignment of alignment angle required that a cell have an aspect ratio greater than the "elongation" threshold of 3.

Pooled elongation and alignment data (three separation experiments) for cells exposed to pre-imprinted grooves and grooves imprinted *in situ* ~6 h. after cell plating ("dynamically imprinted surfaces") are shown in Table 3, and aspect ratios versus absolute alignment angles are plotted for each cell at three different times over ~16 h. in Figure 3. By t = 4.6 h, nearly 70% of cells had elongated (AR > 3), with a significant fraction of these aligned cells displaying long processes (AR ≥ 6). Greater than 80%

of elongated cells (57% of *all* cells) were aligned to grooves (i.e., absolute AA ≤ 15°). Of the cells that were not aligned at 4.6 h., a large majority were also not elongated. Moreover, even at this relatively early time point, few cells were observed with processes extending at angles far from the groove axis (AA > 45°), with no cells in this far-from-axis group having an AR that significantly exceeded the threshold value for elongation. As expected, an increasing fraction of cells plated on pre-imprinted grooves became "aligned" throughout the study. At later measurement times (t = 11.0 h. and t = 16.3 h.), most cells had become bipolar, some with very large aspect ratios, and nearly all elongated cells (94%) were aligned to grooves. Such observations are similar to those reported by other researchers using pre-imprinted grooved substrates [2, 42].

In contrast, on dynamically imprinted surfaces at t = 4.6 h., a smaller fraction of cells were elongated (56%), and only a small majority of elongated cells (and less than one-third of all cells) aligned with grooves. And unlike cells plated on pre-imprinted surfaces, elongated cells on dynamic surfaces showed both a broad range of AA values and a relatively large mean absolute AA value. By t = 11.0 h., a large majority of cells (>80%) were elongated, and nearly 70% of elongated cells were aligned to grooves; nevertheless, the mean absolute AA was twice that for cells plated on pre-imprinted grooves at the same nominal time point (22° vs. 11°). Moreover, although a majority of elongated cells were aligned at both 4.6 h. and 11.0 h., a moderate number of cells extended processes in directions far from the groove axis (absolute AA > 45°) at both time points. At the final time point, t = 16.3 h., nearly all cells had an absolute AA < 30° and the mean absolute AA had decreased to 16° (although the fraction of elongated cells that were aligned did not significantly change from t = 11.0 h.) These findings suggest that, as adherent, polygonal cells adapt to grooves introduced to their existing substrate, they do not initially elongate in an orientation that is necessarily parallel to grooves. This behavior appears to be distinct from that of cells elongating on pre-formed grooves, where the anisotropy of the surface at the time of adhesion appears to determine the direction of initial elongation.

At the final time point measured in these studies, t = 16.3 h., only 6% of elongated cells plated on pre-imprinted substrates had not aligned to grooves. In contrast, 29% of elongated cells on the dynamically imprinted substrates were not aligned, despite this time point representing the *minimum*

exposure time of any given cell to grooves (i.e., most cells had interacted with grooves for more than 16.3 h.). This finding suggests that cells align to grooves less rapidly if they had previously adhered to, and adopted a polygonal morphology on, a planar surface.

Slower alignment of cells on dynamically imprinted surfaces may be a result of barriers to reorganizing subcellular elements that maintain well-defined morphologies. Active remodeling of cell shape and orientation after topographical change requires, for example, disassembly and reassembly of actin filaments and the release and formation of focal adhesions [41]. In contrast, amorphous cells plated onto existing grooves can more immediately respond to the anisotropic surface and dedicate their subcellular machinery to elongation and alignment along grooves [32].

Ebara *et al.* reported using a temperature-switchable shape-memory polymer to promote cell elongation and alignment over 48 h. in response to a transition from planar to grooved topography [42]. Similar to our results, substantial changes in both AR and AA values were observed, with decreased dispersion of AA over the experimental time course. Importantly, however, Ebara's studies required cells to be maintained at 32°C for extended periods in order to take advantage of the ability to induce thermal transitions.

Characterizing how adherent cells respond to de novo stimulation by topographical cues presents unique challenges, requiring new technologies for modifying substrate topographies in real time without perturbing environmental factors, including temperature, that may influence relevant cell behaviors. While systems that undergo substrate changes based on responses of thermally sensitive smart materials provide useful information, the approach described in the current report provides capabilities for presenting adherent cells with dynamic topographic cues without changing ambient temperature, avoiding, for example, modifications to the kinetics of cytoskeletal rearrangement and cell motility [43, 44]. In addition, although not the focus of these initial studies, in situ imprinting should be valuable both in exploring rapid responses of adherent cells to topographic stimulation, as individual tiles can be modified in ~2 min., and in targeting individual cells-of-interest with highly localized, specific topographical changes.

4. Conclusions

We have developed an approach to observe cell morphology and alignment in response to topographical changes introduced to the cell culture substrate. By imprinting protein hydrogel substrates with grooves having an approximate depth of ~2 μm, we can remotely trigger changes in the morphology and alignment of adherent cells while maintaining a uniform temperature. Notably, the kinetics for alignment of elongated cells along the groove dimension proceeds with kinetics significantly slower than for cells plated directly on pre-formed grooves, indicating that cells having existing structured morphologies may be subject to kinetic bottlenecks not experienced by amorphous cells when exposed to topographical triggers for elongation and alignment.

This in situ imprinting approach is a powerful research tool that will enable the study of adherent-cell responses to a range of topographical cues, and could help clarify molecular mechanisms involved in cell motility. We previously reported that changes in stiffness can accompany topographic changes produced by imprinting; however, it is possible to avoid modifications to stiffness, when desired, by empolying protocols that isolate re-scanning from regions in direct proximity to the substrate surface [17]. Understanding the responses of adherent cells to a range of de novo changes in their substrate should provide new insights into mechanisms that underlie complex behaviors such as wound healing and cancer metastasis [45].

Acknowledgements

We gratefully acknowledge discussions with E. T. Ritschdorff and D. S. Hernandez. This work was supported by a grant from The Robert A. Welch Foundation (F-1331).

References

1. Ross A M, Jiang Z, Bastmeyer M, and Lahann J 2012 Physical aspects of cell culture substrates: topography, roughness, and elasticity *Small* **8** 336–55.
2. Curtis A and Wilkinson C 1997 Topographical control of cells *Biomaterials* **18** 1573–83.
3. Discher D E, Janmey P, and Wang Y L 2005 Tissue cells feel and respond to the stiffness of their substrate *Science* **310** 1139–43.
4. Ito Y 1999 Surface micropatterning to regulate cell functions *Biomaterials* **20** 2333–42.
5. Saito A C, Matsui T S, Ohishi T, Sato M, and Deguchi S 2014 Contact guidance of smooth muscle cells is associated with tension-mediated adhesion maturation *Exp Cell Res* **327** 1–11.
6. Tocce E J, *et al.* 2010 The ability of corneal epithelial cells to recognize high aspect ratio nanostructures *Biomaterials* **31** 4064–72.
7. Pot S A, *et al.* 2010 Nanoscale topography-induced modulation of fundamental cell behaviors of rabbit corneal keratocytes, fibroblasts, and myofibroblasts *Invest Ophthalmol Vis Sci* **51** 1373–81.
8. Cox T R, and Erler J T 2011 Remodeling and homeostasis of the extracellular matrix: implications for fibrotic diseases and cancer *Dis Model Mech* **4** 165–78.
9. Barker T H 2011 The role of ECM proteins and protein fragments in guiding cell behavior in regenerative medicine *Biomaterials* **32** 4211–14.
10. Wells R G 2008 The role of matrix stiffness in regulating cell behavior *Hepatology* **47** 1394–1400.
11. Watt F M and Huck W T 2018 Role of the extracellular matrix in regulating stem cell fate *Nat Rev Mol Cell Biol* **14** 467–73.
12. Berg G J, McBride M K, Wang C, and Bowman C N 2014 New directions in the chemistry of shape memory polymers *Polymer* **55** 5849–72.
13. Rico F, Chu C, Abdulreda M H, Qin Y, and Moy 2010 Temperature modulation of integrin-mediated cell adhesion *Biophys J* **99** 1387–96.
14. Tibbitt M W, Kloxin A M, Dyamenahalli K U, and Anseth K S 2010 Controlled two-photon photodegradation of PEG hydrogels to study and manipulate subcellular interactions on soft materials *Soft Matter* **6** 5100–08.

15. Kiang J D, Wen J H, del Alamo J C, and Engler A J 2013 Dynamic and reversible surface topography influences cell morphology *J Biomed Mater Res A* **101** 2313–21.

16. Lam M T, Clem W C, and Takayama S 2008 Reversible on-demand cell alignment using reconfigurable microtopography *Biomaterials* **29** 1705–12.

17. Hernandez D S, Ritschdorff R T, Connell J L, and Shear J B 2018 In situ imprinting of topographic landscapes at the cell-substrate interface, *J. Am. Chem. Soc* **140** 14064–68.

18. Wang J H C, Celechovsky, C, and Woo, S L Y 1999 Effects of silicone microgrooves on 3T3 fibroblasts. *Proc. First Joint BMES/EMBS Conference.* DOI: 10.1109/EMBS.1999.803936.

19. Meyle, J, Gültig, K, Brich, M, Hämmerle, H, and Nisch, W 1994 Contact guidance of fibroblasts on biomaterial surfaces. *J. Mat. Sci.: Mat. Med.* **5**, 463–66.

20. Nielson R, Kaehr B, and Shear J B 2009 Microreplication and design of biological architectures using dynamic-mask multiphoton lithography *Small* **5** 120–25.

21. Kochevar I E, Redmond R W 2000 Photosensitized production of singlet oxygen *Methods Enzymol*. **319** 20–28.

22. Shen HR, Spikes JD, Kopeckova P, Kopecek J 1996 Photodynamic crosslinking of proteins. II. Photocrosslinking of a model protein-ribonuclease A *J Photochem Photobiol B*. **35** 213–19.

23. Verweij H, Van Steveninck J 1982 Model studies on photodynamic cross-linking. *Photochem Photobiol*. **35** 265–67.

24. Schindelin J, *et al.* 2012 Fiji: an open-source platform for biological-image analysis *Nat Methods* **9** 676–82.

25. EllipseFitter.java (University of Washington, Seattle, Washington).

26. Pitts J D, Campagnola P J, Epling G A, and Goodman S L 2000 Submicron multiphoton free-form fabrication of proteins and polymers: Studies of reaction efficiencies and applications in sustained release *Macromolecules* **33**, 1514–23.

27. Basu S, *et al*. 2005 Multiphoton excited fabrication of collagen matrixes cross-linked by a modified benzophenone dimer: Bioactivity and enzymatic degradation, *Biomacromolecules* **6** 1465–74.

28. Allen R, Nielson R, Wise D D, and Shear J B 2005 Catalytic three-dimensional protein architectures *Anal Chem* **77**, 5089–95.

29. Kaehr B, *et al.* 2006 Direct-write fabrication of functional protein matrixes using a low-cost Q-switched laser *Anal Chem* **78** 3198–3202.

30. Weiss P 1929 Erzwingung elementarer Strukturverschiedenheiten am in vitro wachsenden Gewebe *Wilhelm Roux' Archiv für Entwicklungsmechanik der Organismen* **116**, 438–554.

31. Wang J H C, Celechovsky C, and Woo S L Y in *Proceedings of the First Joint BMES/EMBS Conference. 1999 IEEE Engineering in Medicine and Biology 21st Annual Conference and the 1999 Annual Fall Meeting of the Biomedical Engineering Society*, DOI: 10.1109/EMBS.1999.803936.

32. Oakley C, and Brunette D M 1993 The sequence of alignment of microtubules, focal contacts and actin filaments in fibroblasts spreading on smooth and grooved titanium substrata *J Cell Sci* **106** *(Pt 1)* 343–54.

33. Meyle J, Gültig K, Brich M, Hämmerle H, and Nisch W 1994 Contact guidance of fibroblasts on biomaterial surfaces *Journal of Materials Science: Materials in Medicine* **5**, 463–66.

34. Walboomers X F, Ginsel L A, and ansen J A 2000 Early spreading events of fibroblasts on microgrooved substrates *J Biomed Mater Res* **51** 529–34.

35. Ryan G L, Petroccia H M, Watanabe N, and Vavylonis D 2012 Excitable actin dynamics in lamellipodial protrusion and retraction *Biophys J* **102** 1493–1502.

36. Teixeira A I, Abrams G A, Bertics P J, Murphy C J, and Nealey P F 2003 Epithelial contact guidance on well-defined micro- and nanostructured substrates *J Cell Sci* **116** 1881–92.

37. Chicurel M E, Chen C S, and ngber D E 1998 Cellular control lies in the balance of forces, *Curr Opin Cell Biol* **10** 232–39.

38. Geiger B, Spatz J P, and Bershadsky A D 2009 Environmental sensing through focal adhesions *Nat Rev Mol Cell Biol* **10** 21–33.

39. Ritschdorff E T, Nielson R, and Shear J B 2012 Multi-focal multiphoton lithography *Lab Chip* **12** 867–71.

40. Peterbauer T, *et al.* 2011 Dynamics of Spreading and Alignment of Cells Cultured In Vitro on a Grooved Polymer Surface *Journal of Nanomaterials* **10** doi:10.1155/2011/413079.

41. Raghunathan V K, *et al.* 2013 Nuclear and cellular alignment of primary corneal epithelial cells on topography *J Biomed Mater Res A* **101** 1069–79.

42. Ebara M, Uto K, Idota N, Hoffman J M, and Aoyagi T 2014 The taming of the cell: shape-memory nanopatterns direct cell orientation *Int J Nanomedicine* **9 Suppl 1** 117–26.

43. Thurston G and Palcic B 1987 3T3 cell motility in the temperature range 33 degrees C to 39 degrees C *Cell Motil Cytoskeleton* **7** 361–67.

44. Zimmerle C T and Frieden C 1986 Effect of temperature on the mechanism of actin polymerization *Biochemistry* **25** 6432–38.

45. Ananthakrishnan R and Ehrlicher A 2007 The forces behind cell movement *Int J Biol Sci* **3**, 303–17.

Tables

Table 1. Effect of number of scans, and initial scan position (H_0) on final tile height (H_f). H_i represents initial tile height. Scan-dependence studies used an initial start position, H_0 = 14 um (n = 3 specimens); scan-height studies employed double scanning of tiles (n = 6 specimens).

Scans	H_f (µm)	H_f/H_i
0	9.4 ± 0.3	1.00
1	6.8 ± 0.4	0.72
2	5.2 ± 0.3	0.55
3	5.3 ± 0.4	0.56

H_0 (µm)	H_f (µm)	H_f/H_i
8	7.6 ± 0.6	0.81
10	6.2 ± 0.1	0.66
12	6.4 ± 0.9	0.68
14	6.4 ± 0.3	0.68

Table 2. Effect of scan starting position, H_0, on depth of imprinted grooves. Each tile was double scanned with a groove patterns nominally corresponding to 5-μm-wide ridges and 15-μm-wide troughs. Average initial height of all tiles was 9.4 ± 0.3 μm.

H_0 (μm)	Ridge Height (μm)	Trough Depth (μm)
8	9.1 ± 0.2	0.9 ± 0.3
10	9.1 ± 0.5	1.8 ± 0.7
12	8.9 ± 0.5	1.8 ± 0.5
14	9.3 ± 0.6	2.8 ± 0.2

Table 3. Elongation of NIH3T3 cells on pre-formed and in situ imprinted grooves. Time t = 0.0 h. for pre-imprinted and dynamically imprinted substrates is defined in the text. Cells are considered to be elongated when their aspect ratio (AR) exceeds 3.

Pre-imprinted surfaces

Time	Cells	Elongated Cells	Fraction Elongated	Mean AR, Elongated Cells
4.6 h.	42	29	0.69	5.3 ± 1.5
11.0 h.	41	34	0.83	5.0 ± 1.7
16.3 h.	40	31	0.78	6.0 ± 2.6

Dynamically imprinted surfaces

Time	Cells	Elongated Cells	Fraction Elongated	Mean AR, Elongated Cells
4.6 h.	32	18	0.56	4.7 ± 1.6
11.0 h.	32	26	0.81	5.5 ± 2.4
16.3 h.	32	24	0.75	5.2 ± 2.3

Table 4. Alignment of NIH3T3 cells on pre-formed and in situ imprinted grooves. Cells are considered to be aligned when their alignment angle relative to grooves (AA) is less than 15°. At t = 0 h., cells on pre-formed grooves are approximately round and therefore do not have an alignment angle. Cells experiencing dynamically imprinted grooves for the first time display morphologies characteristic of cells grown on planar surfaces, with random orientations. For both pre-imprinted and dynamically imprinted surfaces, the total number of aligned cells decreased in the final measurement as a result of migration of cells from the imprinted surfaces.

Pre-imprinted surfaces

Time	Aligned Cells	Aligned Cells / Elongated Cells	Mean AA, Elongated Cells
4.6 h.	24	0.83	13° ± 15°
11.0 h.	32	0.94	11° ± 13°
16.3 h.	29	0.94	11° ± 8°

Dynamically imprinted surfaces

Time	Aligned Cells	Aligned Cells / Elongated Cells	Mean AA, Elongated Cells
4.6 h.	10	0.56	34° ± 29°
11.0 h.	18	0.69	22° ± 25°
16.3 h.	17	0.71	16° ± 14°

Figures

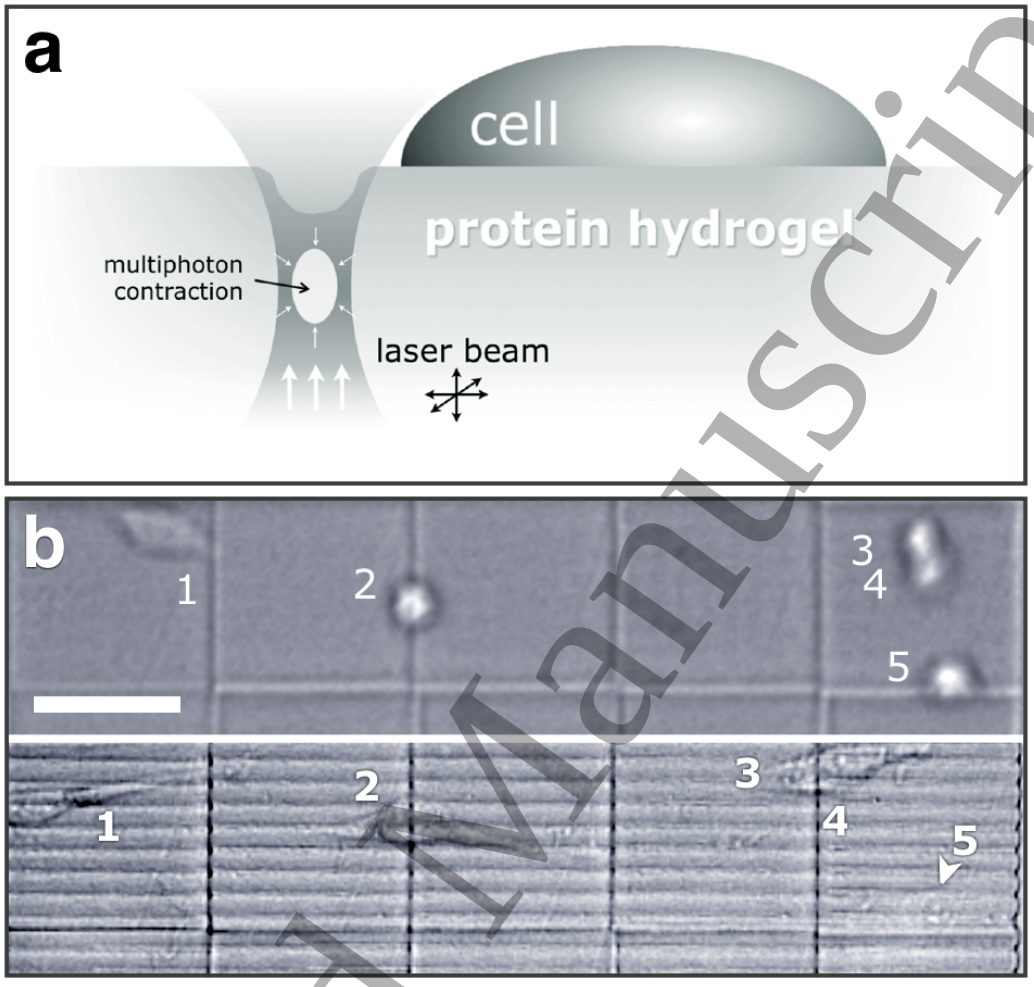

Figure 1. Real time topographic imprinting of a protein-based cell-culture substrate. (a) Multiphoton-promoted crosslinking of the hydrogel substrate within a femtoliter focal volume promotes matrix contraction that projects onto the substrate surface as topographic features. By scanning the laser focus in two or three dimensions, topographic patterns, such as grooves, can be created in real time—even at cell-substrate adhesion sites—to modify cellular behavior. (b) Cell elongation and alignment on a protein-based tile array imprinted with grooves (see also Supporting Movie 1). Top panel: A 10-μm thick gelatin-BSA tile array immediately after settling of cells (identified as 1–5) shortly before imprinting with several micrometer deep grooves. Bottom panel: The same group of cells ~11 h. after imprinting (groove width, 4 μm; pitch, 7-μm) displayed extensive elongation and alignment along the groove axis (cell 5 not readily visible in this image). Scale bar, 50 μm.

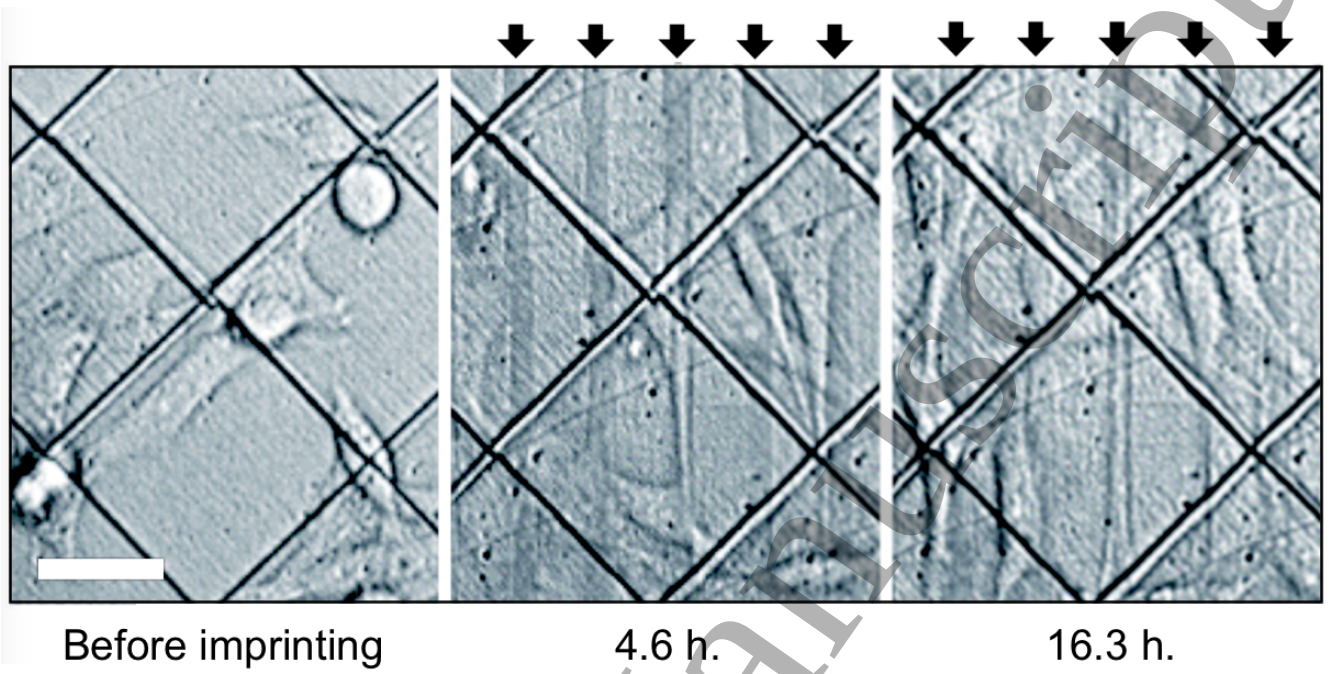

Figure 2. Representative time sequence images of cellular alignment and elongation of NIH3T3 fibroblast cells used to acquire dynamic imprinting response data shown in Tables 3 and 4. Arrows at the top of the middle and right panels identify imprinted grooves; dark diagonal lines are the seams at which printed tiles overlap to form a continuous tile-array substrate. Before imprinting (left panel), most cells display a characteristic random, polygonal morphology; over the ~16 h. of these experiments, cells elongate and generally align to the grooves formed by imprinting. Scale bar, 35 μm.

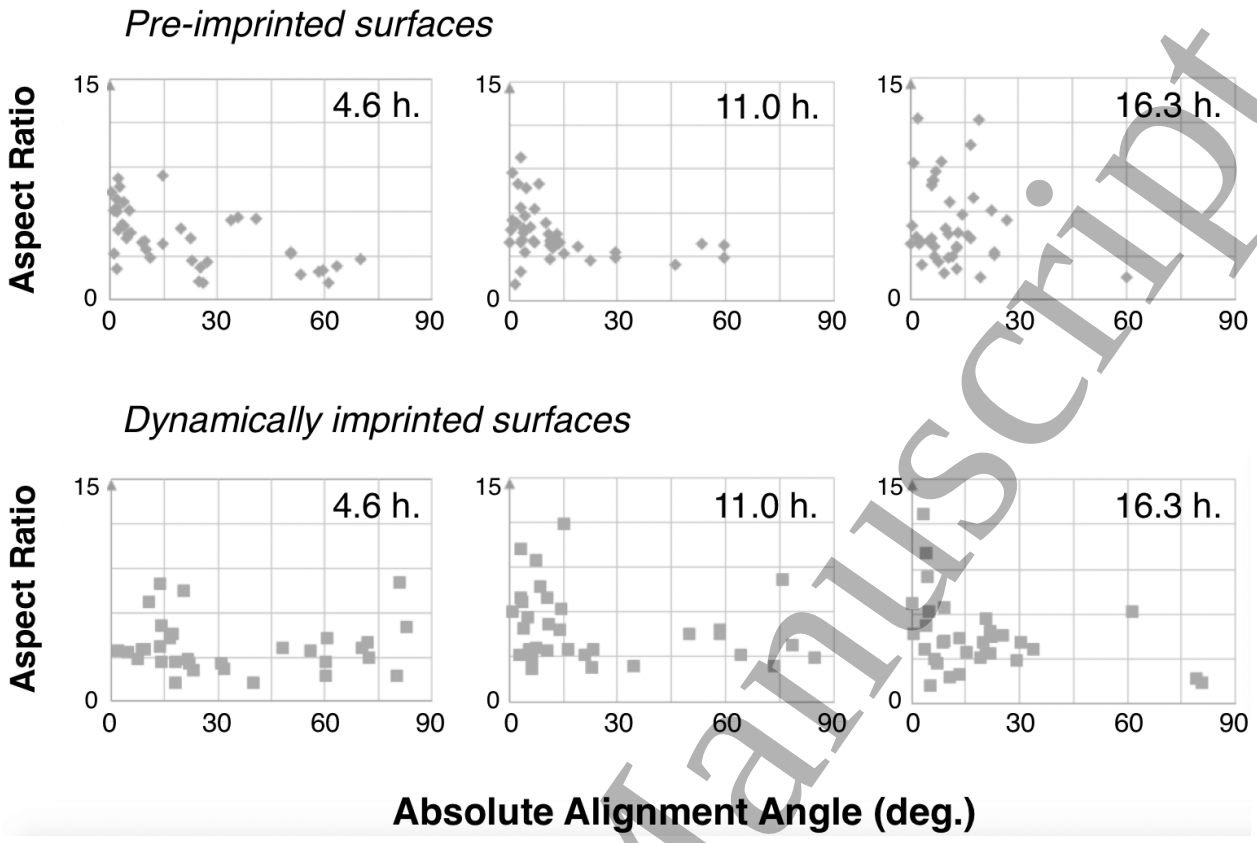

Figure 3. Aspect ratio (AR) vs absolute alignment angle (AA) for individual cells tracked on pre-imprinted grooved surfaces (top) and dynamically imprinted surfaces (bottom) over ~16 h. Number of individual cells analyzed for pre-imprinted and dynamically imprinted surfaces are n = 40 and n = 32, respectively. An AA value of 0° indicates that cells are parallel to grooves. On pre-imprinted surfaces, elongated cells align closely to grooves from early time points, while on dynamically imprinted surfaces cells show a greater spread of absolute alignment angles, particular at shorter times after imprinting.

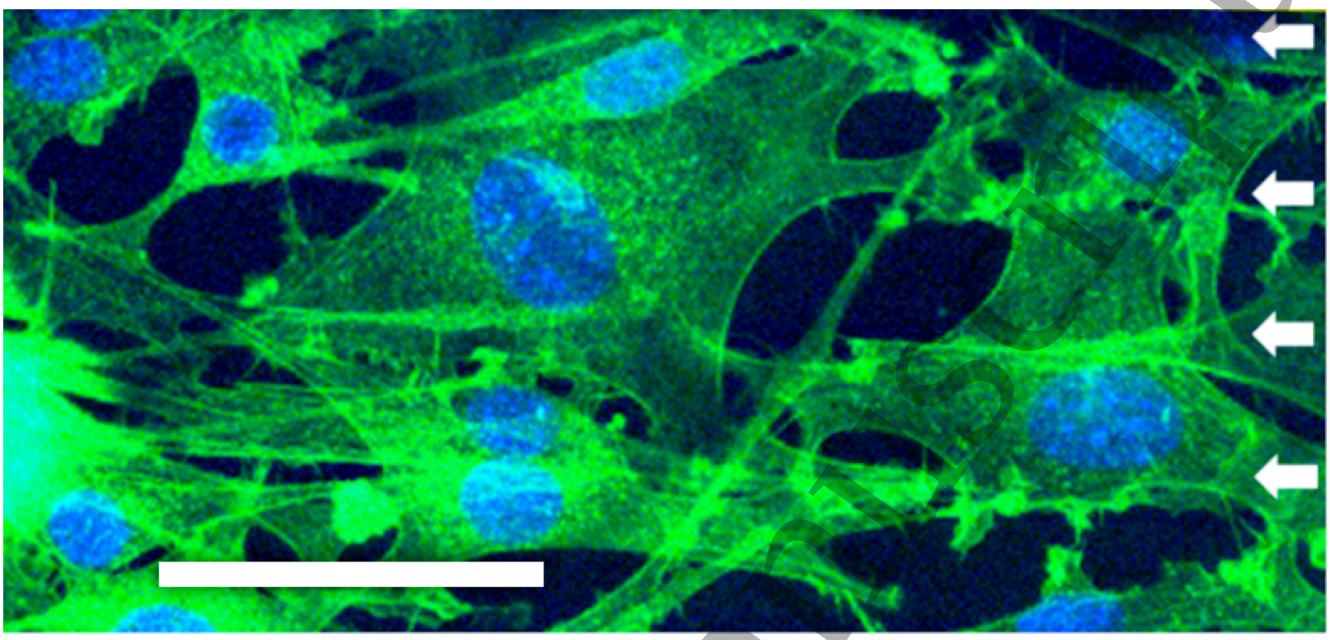

Supplemental Figure S1. Fluorescence image of cells plated on dynamic surfaces. Cells were stained to reveal the location of actin (green), and cell nuclei (blue). The white arrows indicate the locations of the underlying ridges, which are not visible using fluorescence imagain. Substantial alignment of actin to horizontal features demonstrates cell polarization, and oval nuclei indicate mechanotransduction. Scale bar, 70 μm. Methods: Actin filaments of cellular cytoskeletons were stained with Alexa Fluor® 488 Phalloidin (Molecular Probes, Eugene, OR) after formaldehyde fixation. Nuclei were stained with 5 μg/mL solution of 4',6-diamidino-2-phenylindole (DAPI; Molecular Probes, Eugene, OR). Cells were imaged on a confocal microscope (SP2 AOBS, Leica Microsystems, Buffalo Grove, IL) using a 63X (HCX APO, 1.4NA) oil objective. Samples were excited with 405 nm and 488 nm argon lasers. The ranges over which emitted light was collected were 409–483 nm (for DAPI) and 494–515 nm (for Alexa Fluor® 488).